Study on the Effect of Environmental Factors on the Thermal-Atmospheric Environment in Street Canyons

Bin Cheng[a], Songhuan Ma[b], Siqi Wang[b,*], Shuang Liang[a], Chengyang Kang[a], Yiling Deng[c], Lin Jiang[a], Jian Zhang[a]

[a]*Department of Architecture, Southwest University of Science and Technology, Mianyang, China*

[b]*Department of Urban Planning, Southwest University of Science and Technology, Mianyang, China*

[c]*China Chuankai, Chengdu, China*

[*]Corresponding author: wsq@mails.swust.edu.cn

ABSTRACT

The thermal-atmospheric environment is a complex system influenced by various factors. This study explored the impacts of various intricate factors on thermal comfort and air quality within different street environments through field measurements combining with questionnaire. Summer results identified a combined thermal-atmospheric environment threshold (neutral physiologically equivalent temperature (NT): 23.34 ℃; neutral PM2.5 concentration (NC): 14.9 μg/m3) for pedestrian thermal and breathing free. The findings indicated that physical factors exert varying effects on the thermal-atmospheric environment across different street settings. Specifically, more open street spaces tend to be associated with higher temperatures, resulting in elevated physiologically equivalent temperature (PET) values. Yet the land albedo showed little effect. The variation in $PM_{2.5}$C is relatively intricate, being primarily linked to traffic flow. In streets with good air quality, an increase in the sky view factor (SVF) might lead to a rise in $PM_{2.5}$ concentration ($PM_{2.5}$C). Finally, the research aims to help urban planning scholars gain a deeper understanding of the street thermal environment, air quality, and public health in subtropical cities.

KEYWORDS: Thermal-atmospheric environment; physiologically equivalent temperature; $PM_{2.5}$ concentration; sky view factor; albedo; traffic volume

1. Introduction

Global warming, air pollution, and other issues posed serious threats to people's health and satisfaction (Yin et al., 2022). Extreme heatwaves subjected people to heat stress (Wu et al., 2023), which might trigger thermal discomforts, low working efficiency (Liang et al., 2024), and illnesses relating to overheat (Hartz, 2012). Residents needed to rely on mechanical cooling (Atmaca and Gedik, 2019) for thermal adaptation. This consumed large-amount energy (Chamandoust et al., 2020), resulting in air pollutant emission. It can be seen, extreme weathers and atmospheric pollution (Moretti et al., 2013) are interactively impactive. Optimising urban thermal-atmospheric environments has urgent task (Jiang et al., 2024).

Thermal-atmospheric environments (TAEs) could be influenced by various factors (Lai et al., 2019). They could be optimised by proper layout design sustainably. Well forested streets usually had better TAEs since the effects of trees (Salehi and Nasrollahi, 2024). This was performed by sunlight obstruction (Heshani and Winijkul, 2022), heatwave absorption, and atmosphere matter digestion (Chen et al., 2024). Geometric forms of urban spaces were also influential (Cha and Shik, 2020). Sites with higher openness were beneficial in matter release (Wang et al., 2022), purifying the air. However, they also accessed more solar radiation (Xiao et al., 2024), causing more serious heat stress (Mohite and Surawar, 2024). Streets paralleling with local permanent wind direction could enjoy better natural ventilation (Wu et al., 2022), which was beneficial in both thermal comforts and atmosphere .

There were diverse parameters proposed indicating physical environments and TAEs. Physical environments could be indicated by vegetation coverage (Karimi et al., 2020), land surface reflectivity (Zhang et al., 2025b), and sky view factor (SVF, evaluating openness (Zhang et al., 2019b)). The environmental quality (EnQ) was assessed by physiologically equivalent temperature (for thermal comfort) (Ribeiro et al., 2022) and $PM_{2.5}$ concentration ($PM_{2.5}C$ for atmosphere) (Zhu and Lee, 2021). TAEs and environmental parameters were usually statistically correlated with each other (Li et al., 2025a). These findings were directive for urban design in improving TAEs. Zhang et al. (2019a) found that in the park, when the SVF decreased from 0.9 to 0.1, Ta could be decreased by approximately 1.69 °C. Chiang et al. (2023) found that in urban streets, reducing SVF to provide shade can help pedestrians achieve thermal comfort. Additionally, Lee et al. (2024a) found that SVF also affected $PM_{2.5}$. Through ENVI-met simulations, it was discovered that in open spaces with good wind conditions and high radiation levels, temperature increases promoted the diffusion of $PM_{2.5}$. Furthermore, in urban outdoor spaces, different ground reflectance values could be used to regulate the outdoor microclimate. Zhang et al. (2025a) found that in summer, using low-reflectance materials could reduce PET by 3.9 ℃. More importantly, the EnQ was found to influence individual subjective perceptions. Niu et al. (2025) collected pedestrians' thermal sensation votes (TSV) and demonstrated that spatial features, particularly the SVF, significantly affected pedestrians' emotional state and thermal comfort. Luo et al. (2024) further identified air temperature as the most influential external factor governing human thermal sensation, with a marked preference observed for activities in low-SVF environments. Atmospherically, traffic emissions in urban areas contributed to the persistent accumulation of particulate matter (e.g., PM2.5) within street canyons, which not only substantially compromised pedestrian comfort (Li et al., 2025b) but also posed potential health risks (Lee et al., 2024b). Yet the issue could be mitigated by proper design strategies.

Either thermal or atmosphere environment has been widely studied and plenty of important findings acquired. They might be practically impactive. However, there were still some issues unaddressed. Most of reviewed studies focused on one aspect of EnQ, physics (Sharmin et al., 2019) or chemistry (Kim and Park, 2024). They were poorly available in comprehensive environment adjustment. This study attempted to explore the specific physical factor (SVF) on complex contexts (TAEs). It considered diverse factors, including microclimate and atmosphere, which would be further available for comprehensive EnQ improvement. The whole study would processed field monitoring about parameters of TAEs and their influential factors (SVF etc.) to find their interactive statistical correlations.

2. Methodology

2.1. Study area and site selection

Chongqing is located between 105°11'-110°11' East longitude and 28°10'-32°13' North latitude. It has a humid subtropical monsoon climate, which is defined as Cwa according to the Köppen climate classification standard. This study selected 3 typical commercial streets in Chongqing for field measurement. They vary for functions, building distributions, dimensions, and orientations. There were several points of different SVF opted in each street, there are 6 points for every street, totally 18 points (Fig. 1 and Fig. 2). This would cause complex environmental conditions. Physical factors affecting their TAEs are listed in Table 1.

Table 1

Measuring point feature description.

Streets	Street type	Points	SVF	Main pavement materia	Albedo
Sanxia Plaza street (SXP street, EN-WS & E-W)	Pedestrian street	A1	0.17	Stone brick	0.23
		B1	0.32	Stone brick	0.23
		C1	0.56	concrete	0.15
		A2	0.21	Stone brick	0.20
		B2	0.36	concrete	0.15
		C2	0.67	concrete	0.15
Guanyinqiao street (GYQ street, EN-WS & WN-ES)	Vehicle street	A3	0.24	pitch	0.13
		B3	0.42	pitch	0.13
		C3	0.54	Stone brick	0.25
		A4	0.16	Stone brick	0.25
		B4	0.39	pitch	0.17
		C4	0.64	pitch	0.17
Jiefangbei street (JFB street, EN-WS & WN-ES)	Pedestrian - Vehicle street	A5	0.17	pitch	0.10
		B5	0.39	pitch	0.10
		C5	0.51	Stone brick	0.25
		A6	0.19	pitch	0.10
		B6	0.32	pitch	0.10
		C6	0.51	Spitch	0.10

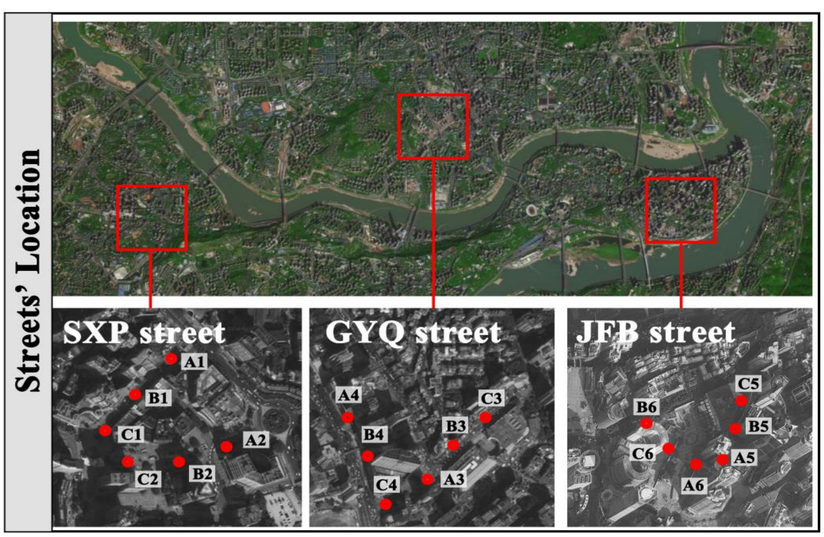

Fig. 1. Location of streets and photos of measurement points.

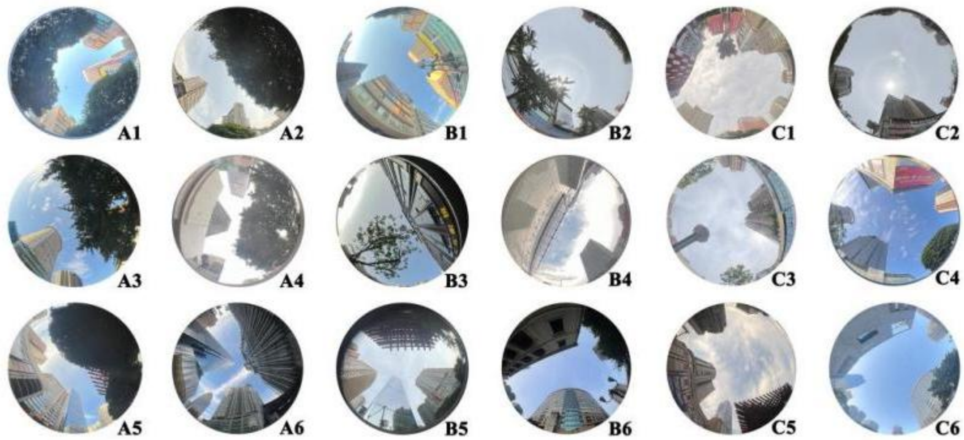

Fig. 2. Point fisheye images.

2.2. Field measurements

The thermal-atmospheric environment parameters were measured at a height of 1.5 meters above the ground with a Testo 400, and the $PM_{2.5}C$ was measured with a BR - SMART. The thermal environment parameters measured in this study consist of air temperature (T_a), globe temperature (T_g), wind speed (V_a), and relative humidity (RH) (Chu et al., 2024; Qin et al., 2024). Each point was measured by one full daytime (8:00 – 20:00). There were two sets of instruments supporting the measurement. Hence, on each day, two points were completely monitored.

2.3. Questionnaire survey

The questionnaire survey randomly targeted to pedestrians in sample streets in the CBD of Chongqing. The questionnaire adopted a structured design and consisted of two parts: The first part collected socio-demographic characteristics and clothing information, including fabric type and coverage (estimated in clo values). The second part was the street thermal environment assessment module (Table 2), which used a 9-point scale (-4 to +4) for thermal sensation vote (TSV), and used a 7-point scale (-3 to +3) for air quality sensation vote (AQSV), and with all perceptual measurements recorded to a precision of 0.1 units. The survey employed stratified random sampling and yielded 1,684 valid responses.

Table 2
TSV scale (Ali and Patnaik, 2018) and AQSV scale (Yin et al., 2022).

Scale	**TSV**	**AQSV**
-4	Extremely cold	-
-3	Cold	Extremely polluted
-2	Cool	Polluted
-1	Slightly cool	Slightly polluted
0	Neutral	Moderate
1	Slightly warm	Slightly fresh
2	Warm	Fresh
3	Hot	Extremely fresh

4	Extremely hot	-

2.4. Indices of TAEs

This study applied various parameters to indicate TAEs. Thermal and atmospheric environments were assessed by PET and $PM_{2.5}$C respectively. Physiologically equivalent temperature is the most widely used indicator. It is based on the Münchner Energiebilanz Modell (MEMI) and calculates the energy exchange between the human body and the environment, converting complex meteorological conditions into an intuitive temperature value (Höppe, 1999). This study uses the *Rayman* model to calculate PET, which typically involves microclimate parameters such as Ta, Va, RH, and MRT, with MRT calculated (Su et al., 2024) as shown in Eq. 1. Additionally, the calculation process involves human metabolic rate or clothing parameters, typically using a standardised human model (Sharmin et al., 2019): height 1.75 m, weight 75 kg, basal metabolic rate approximately 80 W/m², and clothing thermal resistance 0.9 clo.

Typically, PET is often influenced by urban geometry (e.g., SVF, street orientation) and surface reflectance. Higher PET levels are found in more open areas with lower surface reflectance (McRae et al., 2020). In street canyons, $PM_{2.5}$ is directly affected by pollution sources (e.g., traffic flow) and wind conditions, with more air pollutants deposited in calm zones near major roads (Mobarhan et al., 2024).

$$MRT = \left[\left(T_g + 275.15\right)^4 + \frac{1.1\times10^8\cdot v^{0.6}}{\varepsilon\cdot D^{0.4}}\left(T_g - T_a\right)\right]^{0.25} - 273.15 \qquad \text{Eq. 1}$$

Where: Ta is the air temperature (℃); Tg is the global temperature (℃); Va is the air velocity (m/s); D is the diameter of the sphere (0.15 m); and ε is the absorption rate of the Earth (0.95). At the same time, the $PM_{2.5}$ concentration ($PM_{2.5}$C) was applied to indicate the air quality in cities. It has been approved having a significant impact on human health, the environment, and the economy (Kim and Park, 2024). Its concentration level reflects the pollution level of street canyons. Therefore, this paper used $PM_{2.5}$C as the index to evaluate the atmospheric environment of sample streets.

2.5. Factors affecting thermal-atmospheric environment

TAEs are affected by various factors complexly. They were considered in this study as variables. In addition to SVF, albedo is thermal influential. Traffic flow would be influential on atmospheric pollutant concentration. SVF is a normalized index (0 to 1) that represents the sky visibility ratio at a given point, reflecting the extent of sky obstruction caused by surrounding structures (e.g., urban features, vegetation, or topography) .This study used fisheye photography to obtain the SVF of the measurement points (Miao et al., 2020). Specifically, the WinsCANOPY model was used to calculate the processed fisheye images (Fig. 3). The SVF was usually positive correlating (Zhang et al., 2019b) with heat stress but negative correlating with atmospheric pollutants (Wang et al., 2022).

Surface material determines its reflectance. Surface reflectance refers to the ability of the surface to reflect incident shortwave solar radiation, typically expressed as a value or percentage between 0 and 1 . It is usually calculated using Eq. 2.

$$\alpha = \frac{Reflected\ \ Shortwave\ \ Radiation}{Incoming\ \ Shortwave\ \ Radiation} \qquad \text{Eq. 2}$$

Moreover, there were other influential factors, this study applied traffic flow (passing vehicles in united minutes) and current meteorological condition (wind & humidity) for multiple model establishments.

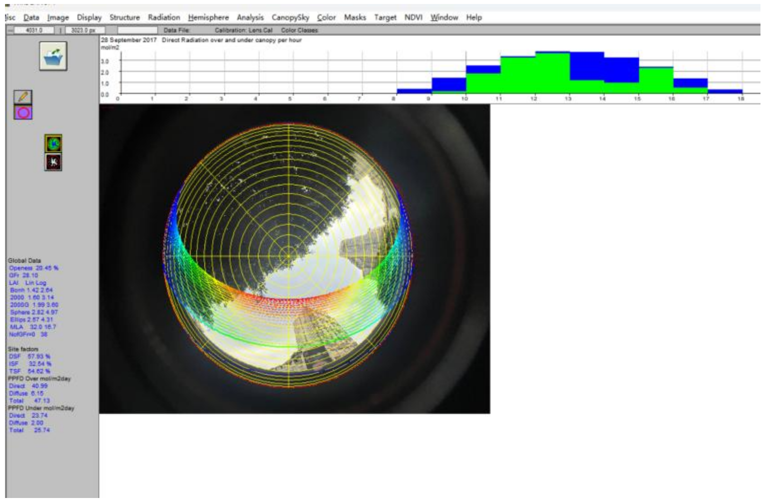

Fig. 3. SVF calculation using WinSCANOPY

2.6. Data analysis

This study used the MLR (Multiple Linear Regression) method to build multiple linear models. The indices of TAEs would be available as dependent variables while their affecting (physical) factors were independen. Specifically, one model examined the relationship between PET and SVF, Albedo, and Ta, with PET as the dependent variable and SVF, Albedo, and T_a as the independent variables. Another model examined the relationship between $PM_{2.5}C$ (dependent variable) and SVF, V_a, RH, and average traffic flow (independent variables).

3. Results

3.1. Subjective responses toward various EnQ parameters in the sample sites

Humans are perceptively affected by thermal environments. This could be explained by the significant linear correlations between thermal sensation and thermal indices. The linear relationships between PET and TSV in street canyons of different ranges are expressed in Fig. 4. They all showed significant positive correlations since high R^2 values (above 0.65). This exported neutral temperatures of 23.34 ℃. That of the of the SXP, GYQ, and JFB streets were 23.53 ℃, 23.49 ℃, and 23.57 ℃, respectively. They were insignificantly different but very close. This suggested that humans' thermal perceptions in summer may not be affected by the type of street.

Atmospheric pollutants are influential on people's health. Respondents might be sensitive with their concentrations. The AQSV was linearly associated with PM2.5C in various scopes. Compared with thermal sensations, they were relative poor negative correlating. People might be poorly perceptive with matters in the air although they are significantly Chealth-impactive (R^2<0.2). This could roughly predict NC values of 14.9 (total), 11.38 (SXP street), 20.31 (GYQ street), 9.09 (JFB street) μg /m^3.

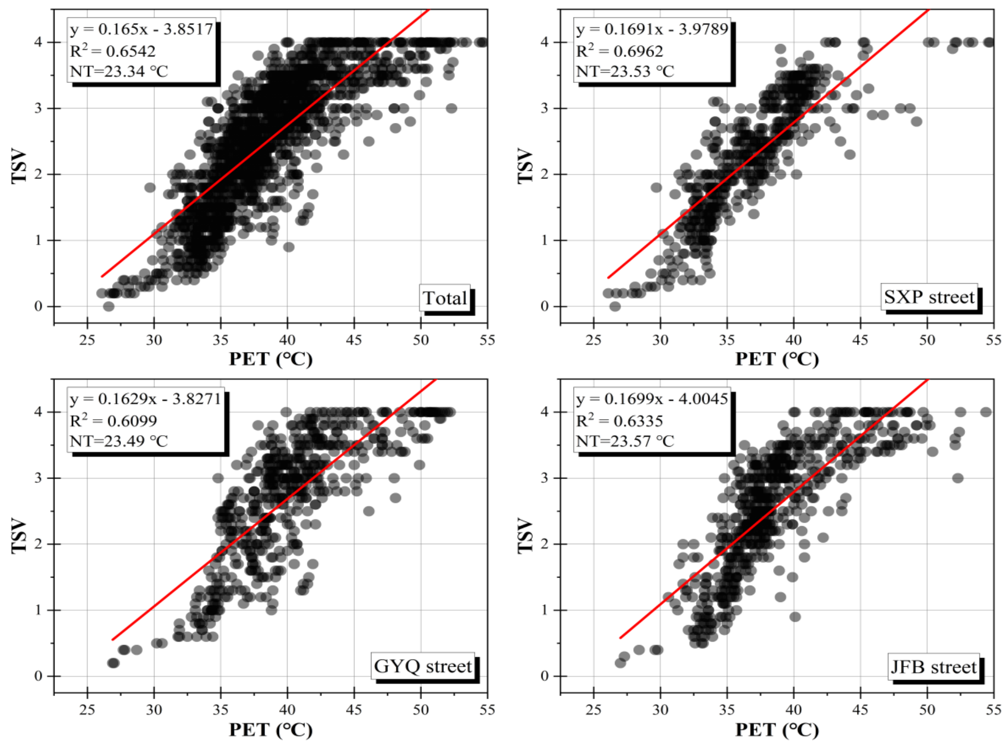

Fig. 4. Linear relationship between PET and TSV in street canyons.

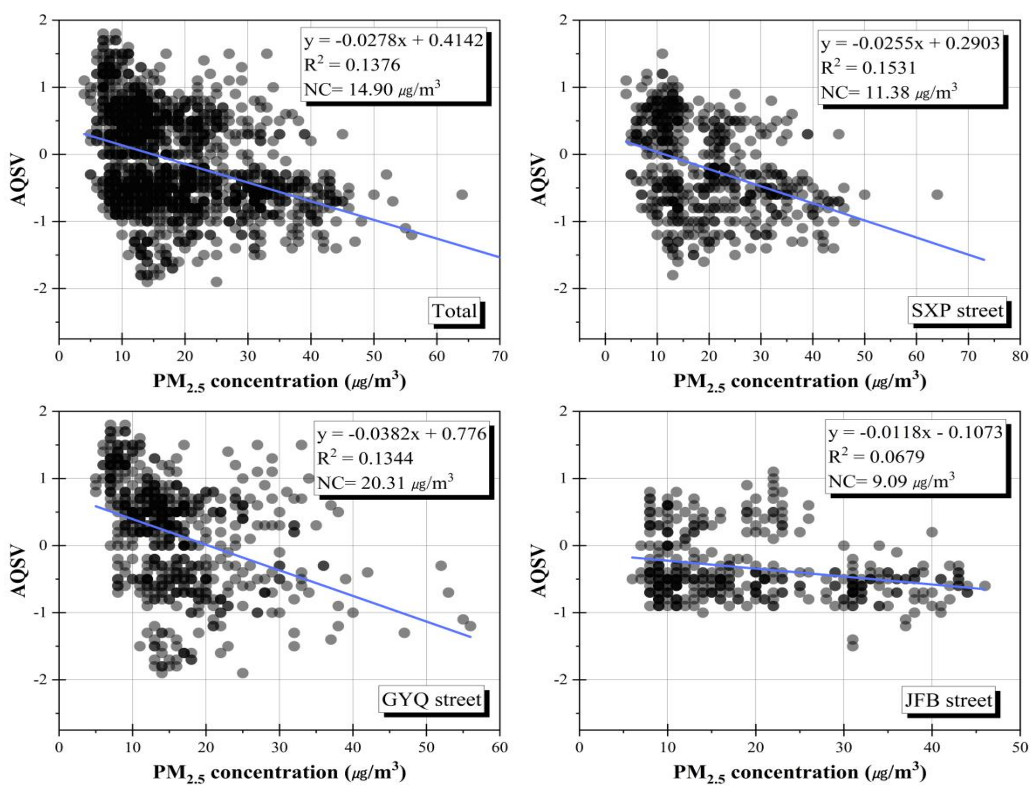

Fig. 5. Linear relationship between $PM_{2.5}C$ and AQSV in street canyons.

3.2. Environmental factors affecting PET

PET was associated with its corresponded affecting factors by multiple linear models (Table 3). Data in various contexts were analysed in separation. This helped to compare the performances of physical factors under various conditions. There were slight differences between results in various locations. Overall, the SVF expressed positive effects with thermal stress. The swell of SVF by every 0.1 point resulted in PET ascent of 0.21 ℃. Compared with either single street, the strongest effect waswitnessed SXP street (SVF increase by every 0.1 resulted in PET ascent of 0.75 ℃), which stronger than JFB street (SVF increase by every 0.1 resulted in PET ascent of 0.69 ℃). Nonetheless, the GYQ street showed totally different trend, the higher temperature was even witnessed sites lower SVF (SVF increase by every 0.1 resulted in PET descent of 0.13 ℃). Yet the albedo presented thermal effects with confusion. There were both positive and negative coefficients emerging.

Table 3

Multiple linear regression models of PET vs. SVF, Albedo, Ta.

	PET vs. SVF, Albedo, T_a	***R^2***
Model 1	$PET_{Total} = 2.064 \times SVF^{***} - 4.125 \times Albedo^{***} + 1.206 \times T_a{}^{***} - 5.905$	0.840
Model 2	$PET_{SXGC} = 7.528 \times SVF^{***} + 17.942 \times Albedo^{***} + 1.577 \times T_a{}^{***} - 24.646$	0.785
Model 3	$PET_{GYQ} = -1.34 \times SVF^{***} - 4.637 \times Albedo^{***} + 1.213 \times T_a{}^{***} - 5.714$	0.963
Model 4	$PET_{JFB} = 6.941 \times SVF^{***} + 0.209 \times Albedo + 1.521 \times T_a{}^{***} - 19.07$	0.841

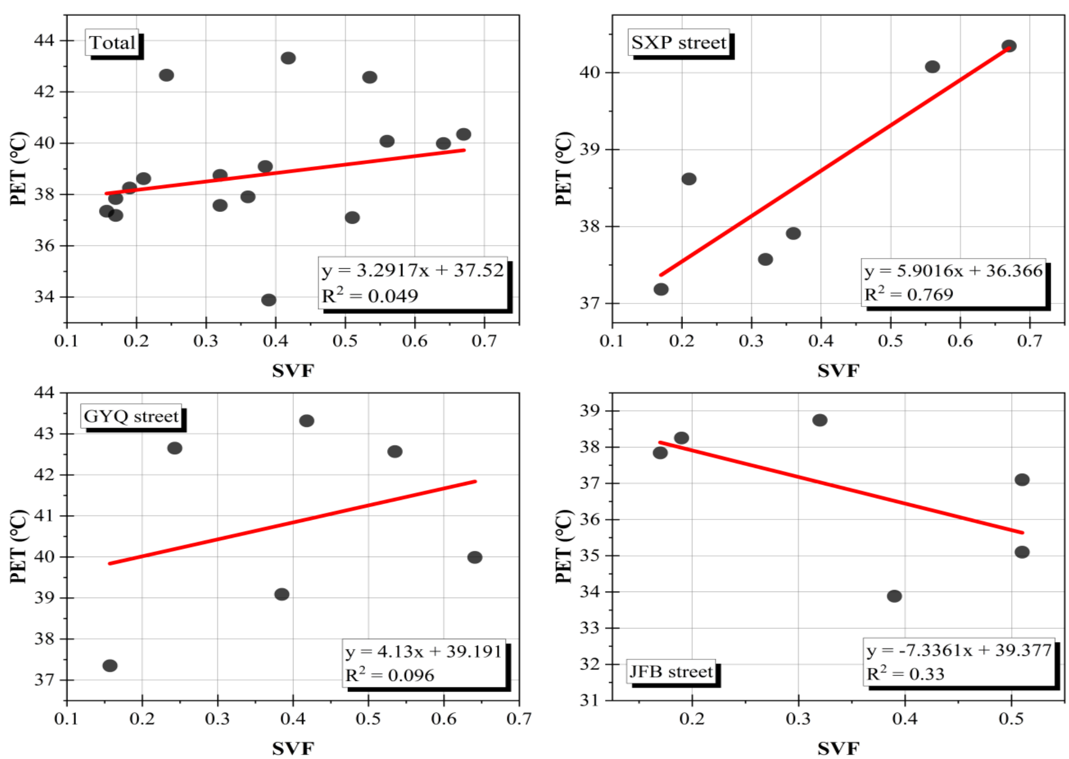

Fig. 6. Linear correlations between SVF and PET average value.

For further exploring the effects of them, Bayesian models were established, which is shown in Fig. 6 and Fig. 7. It can be seen, SVF mostly expressed positive correlations and albedo was poor (negative) associated. Increasing SVF by 0.15 point could cause PET change by 10 ℃. The albedo showed very poor effects. For a single street, The PET on the SXP street was most affected by SVF and reflectivity (k_{SVF}=5.9016, k_{Albedo}=-24.053). In contrast, the least influential utility is located on JFB street (k_{SVF}=-7.3361, k_{Albedo}=-13.761). That is to say, in sample sites, thermal environments were more significantly affected by solar radiation, rather than land reflectivity. The physical factors have created minimum PET values of 34 ℃, which is higher than neutral values calculated in Section 3.1 (23.34 ℃). Physical factors involved by this study were hard to adjust meteorology meeting people's physiological needs independently.

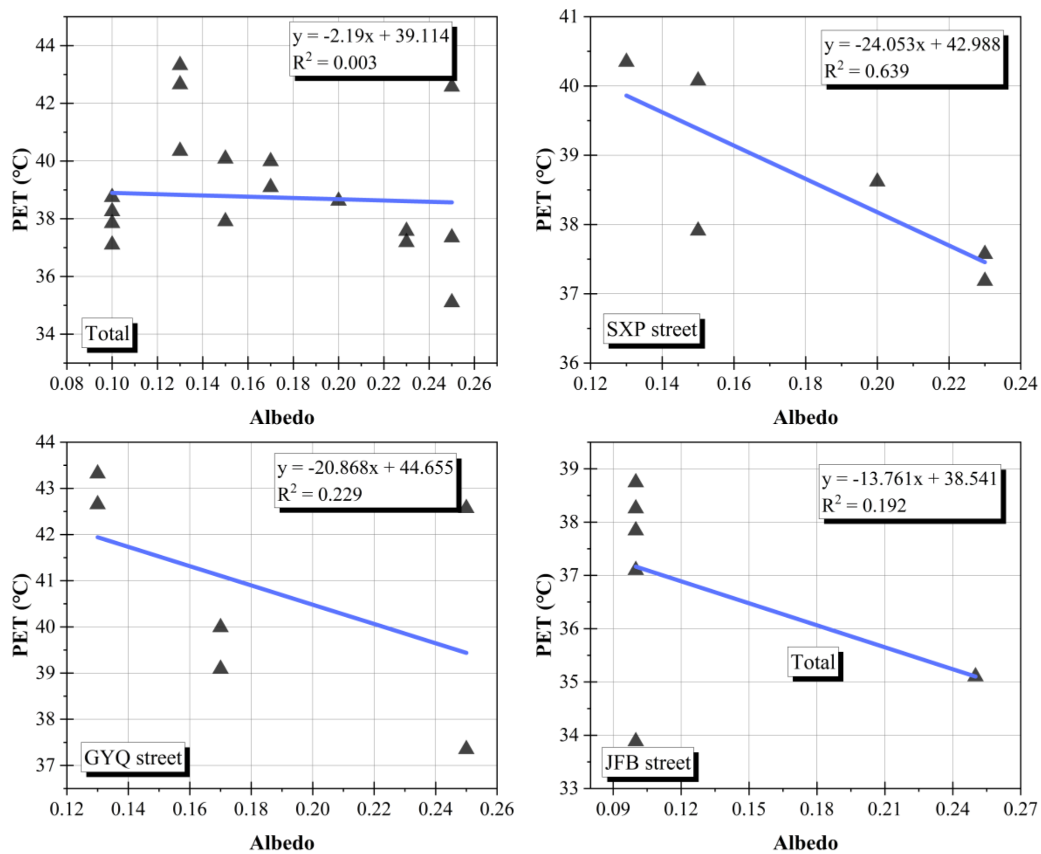

Fig. 7. Linear correlations between Albedo and PET average value.

3.3. Environmental factors affect $PM_{2.5}$ concentration

The air quality index was associated with its influential factors by multiple models (**Error! Reference source not found.**). It can be seen, all relevant factors showed slight different effects, despite of similar overall trends. Either SVF or traffic flow were positively correlated with $PM_{2.5}$C. It was also affected by current meteorology. the whole site, rising SVF by every 0.1 point contributed to $PM_{2.5}$C ascent above 2.20 μg/m^3. Similar results were witnessed in SXP street (SVF increase by every 0.1 resulted in $PM_{2.5}$C ascent of 3.36 μg /m^3) and JFB street (SVF increase by every 0.1 resulted in $PM_{2.5}$C ascent of 3.97 μg /m^3). However, it was insignificantly influential in GYQ street (SVF increase by every 0.1 resulted in $PM_{2.5}C$ ascent of 0.17 μg /m^3). Vehicles are the essential resources of atmospheric pollution, average traffic volume increase by 10 point every 6 minutes contributed to $PM_{2.5}C$ ascent above 5 μg /m^3. Therefore, it was equally influential in all ranges. To some extent, $PM_{2.5}C$ could be affected by meteorology. The wind is capable to disperse the matter in the atmosphere.

Table 4

Multiple linear regression models of $PM_{2.5}C$ vs. SVF, V_a, RH, average traffic volume.

	$PM_{2.5}C$ vs. SVF, V_a, RH, average traffic volume (per 6 min)	***R^2***
Model 5	$PM_{2.5}C_{Total} = 21.96 \times SVF^{***} - 0.473 \times Va + 0.39 \times RH^{***} + 0.501 \times traffic\ \ flow^{***} - 20.479$	0.476
Model 6	$PM_{2.5}C_{SXGC} = 33.664 \times SVF^{***} - 0.631 \times Va \quad + 0.39 \times RH^{***} + 0.428 \times traffic\ \ flow^{***} - 16.143$	0.605
Model 7	$PM_{2.5}C_{GYQ} = 1.675 \times SVF \quad - 1.255 \times Va^{*} + 0.21 \times RH^{***} + 0.655 \times traffic\ \ flow^{***} - 7.175$	0.402
Model 8	$PM_{2.5}C_{JFB} = 39.721 \times \mathrm{SVF}^{***} - 0.316 \times Va + 0.246 \times RH^{***} + 0.61 \times traffic\ \ flow^{***} - 16.143$	0.653

For enhanced understanding of these relationships, we employed Bayesian statistical models, which is shown in Fig. 8 and Fig. 9. It can be seen, SVF and traffic volume both mostly expressed positive correlations. Increasing SVF by about 0.14 point could cause $PM_{2.5}C$ change by 10 μg /m^3. Contrary to typical patterns, higher SVF values in GYQ street correlated with lower PET. Additionally, the traffic volume exhibited a stronger effect, overall, increasing the average traffic volume by about 2 point could cause $PM_{2.5}C$ change by 10 μg /m^3. For a single street, The $PM_{2.5}C$ on the JFB street was most affected by SVF and average traffic volume (k_{SVF}=0.0168, $k_{traffic\ volume}$=0.1734). In comparison, the least influential utility was located on GYQ street (k_{SVF}=-0.0125, $k_{traffic\ volume}$=0.2365). This signifies that more open areas did not necessarily indicate lower air pollution levels, as $PM_{2.5}$ background level had to be must be taken into account. The minimum values (9.5 μg /m^3) were within individual sensation ranges (14.9 μg/m^3).

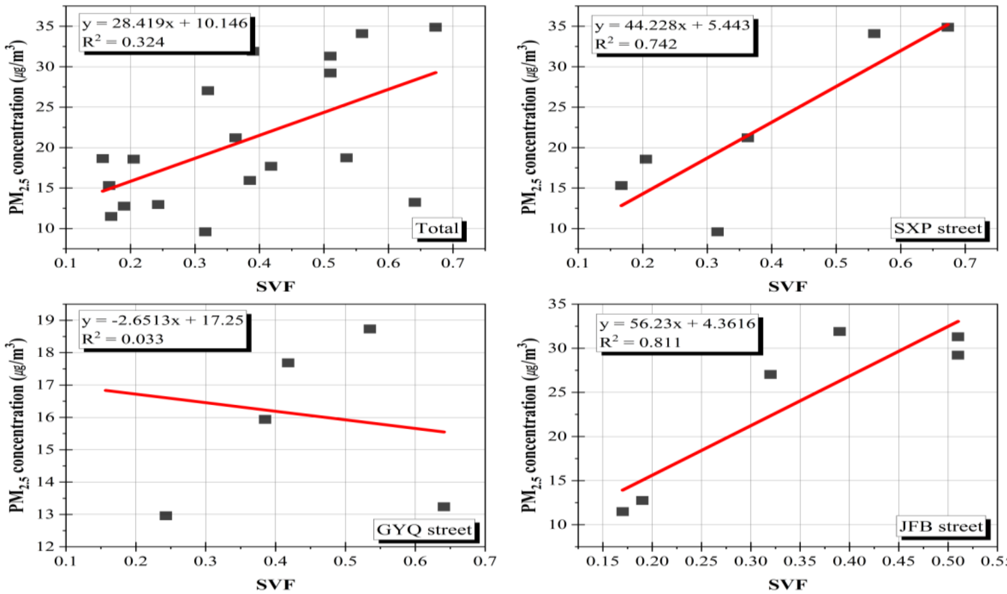

Fig. 8. Linear correlations between SVF and $PM_{2.5}C$ average value.

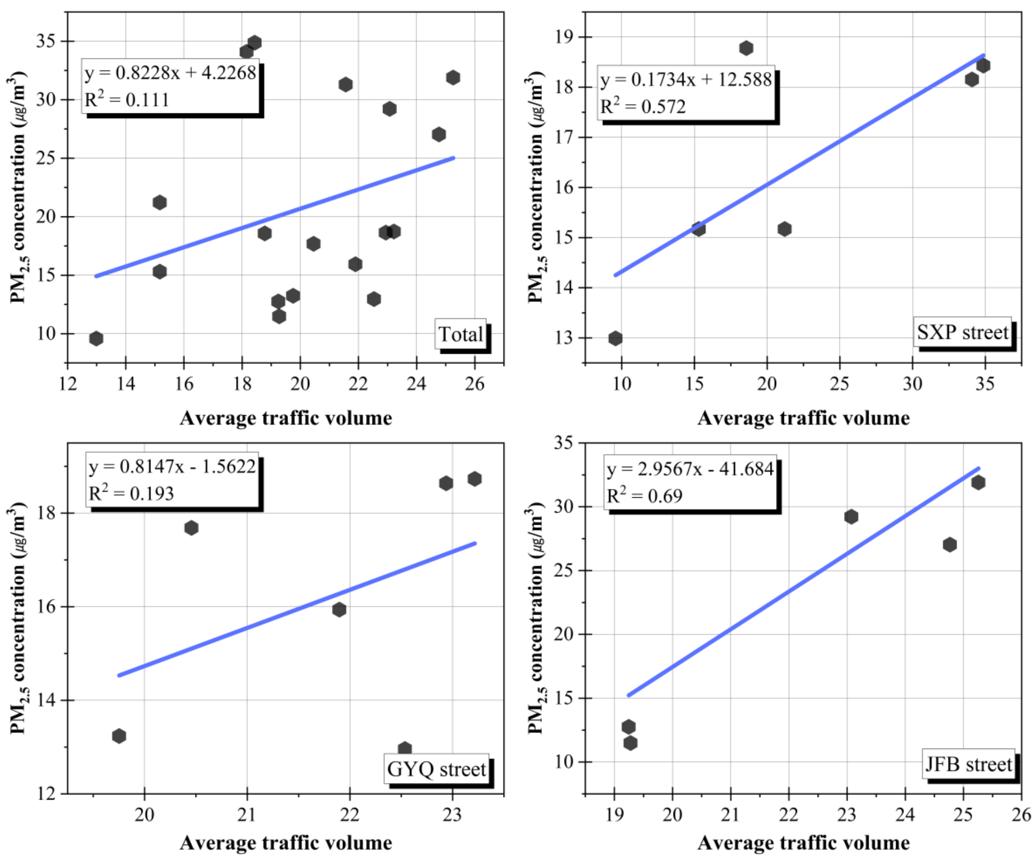

Fig. 9. Linear correlations between average traffic volume and $PM_{2.5}C$ average value.

4. Discussion

This study has investigated effects various factors. Some its echoed that earlier studies whilst others conflicted. They could be explained by some scientific principles.

This study found that Chongqing has exhibited a relatively low neutral temperature compared with other cities in same climate zones. Humans' thermal perceptions attributed to the long-term effects of thermal history (Lam et al., 2021b). High temperatures make pedestrians more sensitive to EnQ (Dong et al., 2020), particularly in areas with high-density building layouts (Zhan et al., 2024). This phenomenon compels pedestrians to actively adapt to extreme climatic conditions (Lam et al., 2021a), thereby resulting in a downward shift in the neutral temperature threshold (Huang et al., 2023). Nevertheless, the phenomenon by this study was opposite with that, this shows local people's poor thermal tolerance.

In terms of thermal environment, SVF was the main factor affecting the thermal comfort of pedestrians. The more open the space, the more solar radiation the ground received, making the pedestrian PET rise (Li et al., 2020). Secondly, compared with the dark ground with low reflectivity, some light-colored pavement (such as light-colored asphalt, white stone bricks) was able to reflect solar radiation to a certain extent, so as to reduce the temperature (Huang et al., 2020). In the street design planning, it should have been recommended to adopt light-colored materials for ground painting, arrange squares at street entrances and exits or in the middle position. Nevertheless, albedo exhibited poorer effects compared to SVF. This finding conflicted with the investigations revealing thermal adjusting of land reflectivity (Liu et al., 2024). This study conducted the field survey on pavements paralleling with vehicle roads. They might have been covered by similar materials with slight reflectivity variation (Krispel et al., 2019). Also, the albedo affected thermal environments passively (Zhang et al., 2025a), which was different from SVF (Shata et al., 2021). Hence, it was revealed that thermal stresses in sunny summer days were more significantly affected by direct sunlight radiation.

In terms of air quality, compared with the thermal environment, SVF had a negative effect, because the initial value of $PM_{2.5}C$ on the street was very low (about 10-20 μg /m³), and $PM_{2.5}$ in the surrounding environment was concentrated there by making the space more open (Fu et al., 2017). The average traffic flow on the street was the main way to reduce $PM_{2.5}C$ (Zhong et al., 2024), and the high relative humidity promoted the formation of particles(Miao et al., 2023), therefore, Controlling traffic flow could effectively reduce the accumulation of $PM_{2.5}$ in the street canyons of hot - humid cities. However, some unusual finding should not be neglected. SVF mostly positively correlated with $PM_{2.5}C$ in this study. As to general conditions, higher open space (larger SVF) would enjoy better nature ventilation (Li et al., 2022), improving air quality (Liu et al., 2021). This was also approved by the effects of air velocity. Nevertheless, this study revealed an unexpected phenomenon where areas with higher openness exhibited elevated $PM_{2.5}C$. This counterintuitive finding could be explained by the ventilation effect in open street canyons: when background $PM_{2.5}$ levels were low, the well-ventilated conditions facilitated the transport and accumulation of air pollutants from adjacent high-pollution areas, ultimately increasing local $PM_{2.5}C$ (Fu et al., 2017). Section 3.2 has expressed that thermal environments created by the SVF and high albedo were higher people's neutral values. Hence it is hard to meet the needs of thermal adaptation relaying openness and land reflectivity only. Other factors, such as vegetation, are needed as compensations.

Findings of this study would be practically impactive. Future urban planning and design works could be directed in EnQ improvement. Limitations of this study should not be ignored. There were plenty of factors affecting TAEs. Some of them (e.g., trees) were not considered by this study. Consequently, thermal environments created by low SVF were beyond people's preferences. These shortages should be addressed in future studies.

5. Conclusion

This study has investigated physical factors affecting thermal-atmosphere environmental conditions field monitoring. There were some important findings acquired. They were listed follows.

Pedestrians attained a summer neutral thermal sensation at a of 23.34 ℃ (PET) and a $PM_{2.5}C$ of 14.9 μg/m^3.

Daytime thermal environments were more significantly impacted by site openness, rather than land reflectivity; each 0.1 increase in SVF led to a 0.21 ℃ rise in PET; since thermal stress of sample might be more resulted from solar radiation.

In street canyons, SVF emerged as the primary factor influencing $PM_{2.5}C$, where each 0.1 point increase in SVF led to a $PM_{2.5}C$ rise exceeding 2.20 μg/m^3. However, traffic flow patterns equally constituted a significant determinant, demonstrating an overall trend wherein every 10-unit increase in average traffic volume per 6-minute interval elevated $PM_{2.5}$ concentrations by over 5 μg /m^3. The effects of weather should not be ignored, each 1% increase in RH led to a 0.39 μg/m^3 rise in $PM_{2.5}C$; each 1 m/s increase in V_a contributed to a 0.47 μg /m^3 decrease in $PM_{2.5}C$.

Findings of this study would be practically implicative, in EnQ improvement, future urban design works could be conducted regarding street functions and local climate.

Finding support

This study was financially supported Engineering Research Center of Chuanxibei RHS construction at Mianyang Teachers' College of Sichuan Province with the case number of RHS2024-B8.

References

Ali SB and Patnaik S (2018) Thermal comfort in urban open spaces: Objective assessment and subjective perception study in tropical city of Bhopal, India. Urban Climate 24: 954-967.

Atmaca AB and Gedik GZ (2019) Evaluation of mosques in terms of thermal comfort and energy consumption in a temperate-humid climate. Energy and Buildings 195: 195-204.

Cha S-Y and Shik OK (2020) The Impact of the Geometry of Urban Residential Street Canyons on Thermal Comfort. Journal of the Architectural Institute of Korea 36(12): 187-198.

Chamandoust H, Derakhshan G, Hakimi SM and Bahramara S (2020) Tri-objective scheduling of residential smart electrical distribution grids with optimal joint of responsive loads with renewable energy sources. Journal of Energy Storage 27.

Chen X, He J, Han M, et al. (2024) Understanding the impacts of street greening patterns and wind directions on the dispersion of fine particles. Science of the Total Environment 953.

Chiang Y-C, Liu H-H, Li D and Ho L-C (2023) Quantification through deep learning of sky view factor and greenery on urban streets during hot and cool seasons. Landscape and Urban Planning 232: 104679.

Chu Z, Li S, Li T, et al. (2024) Numerical simulation of layout and landscape elements on the thermal environment of urban squares. Ecological Informatics 82.

Dong J, Peng J, He X, et al. (2020) Heatwave-induced human health risk assessment in megacities based on heat stress-social vulnerability-human exposure framework. Landscape and Urban Planning 203: 103907.

Fu X, Liu J, Ban-Weiss GA, et al. (2017) Effects of canyon geometry on the distribution of traffic-related air pollution in a large urban area: Implications of a multi-canyon air pollution dispersion model. Atmospheric Environment 165: 111-121.

Hartz D (2012) Heat-related Morbidity and Thermal Comfort: A Comparison Study of Phoenix and Chicago. Dissertation/Thesis.

Heshani ALS and Winijkul E (2022) Numerical simulations of the effects of green infrastructure on PM2.5 dispersion in an urban park in Bangkok, Thailand. Heliyon 8(9).

Höppe P (1999) The physiological equivalent temperature e a universal index for the biometeorological assessment of the thermal environment. Int. J. Biometeorol. DOI: 10.1007/s004840050118.: 71-75.

Huang X, Yao R, Xu T and Zhang S (2023) The impact of heatwaves on human perceived thermal comfort and thermal resilience potential in urban public open spaces. Building and Environment 242: 110586.

Huang Z, Gou Z and Cheng B (2020) An investigation of outdoor thermal environments with different ground surfaces in the hot summer-cold winter climate region. Journal of Building Engineering 27.

Jiang L, Yang Y, Wu Q, et al. (2024) Hotter days, dirtier air: The impact of extreme heat on energy and pollution intensity in China. Energy Economics 130.

Karimi A, Sanaieian H, Farhadi H and Norouzian-Maleki S (2020) Evaluation of the thermal indices and thermal comfort improvement by different vegetation species and materials in a medium-sized urban park. Energy Reports 6: 1670-1684.

Kim H and Park EH (2024) Effects of chemical composition of ambient PM2.5 measured in Seoul on potential health risks and generation of reactive oxygen species. Environmental Pollution 352.

Krispel S, Peyerl M, Maier G, et al. (2019) Reduction of Urban Heat Islands with Whitetopping. Cement Wapno Beton 24(3): 173-+.

Lai D, Liu W, Gan T, et al. (2019) A review of mitigating strategies to improve the thermal environment and thermal comfort in urban outdoor spaces. Science of the Total Environment 661: 337-353.

Lam CKC, Cui S, Liu J, et al. (2021a) Influence of acclimatization and short-term thermal history on outdoor thermal comfort in subtropical South China. Energy and Buildings 231: 110541.

Lam CKC, Gao Y, Yang H, et al. (2021b) Interactive effect between long-term and short-term thermal history on outdoor thermal comfort: Comparison between Guangzhou, Zhuhai and Melbourne. Science of the Total Environment 760: 144141.

Lee J, Barquilla CAM, Park K and Hong A (2024a) Urban form and seasonal PM2.5 dynamics: Enhancing air quality prediction using interpretable machine learning and IoT sensor data. Sustainable Cities and Society 117.

Lee S, Tian D, He R, et al. (2024b) Ambient air pollution exposure and adult asthma incidence: a systematic review and meta-analysis. The Lancet Planetary Health 8(12): e1065-e1078.

Li G, Ren Z and Zhan C (2020) Sky View Factor-based correlation of landscape morphology and the thermal environment of street canyons: A case study of Harbin, China. Building and Environment 169.

Li J, You W and Ding W (2022) Exploring urban space quantitative indicators associated with outdoor ventilation potential. Sustainable Cities and Society 79.

Li J, Zhao Z, Chen H and Fu Z (2025a) Study on the microclimate and thermal comfort of urban parks under arid climate conditions: A case study of Shihezi City. Case Studies in Thermal Engineering 71.

Li W, Tian L, Jin X, et al. (2025b) Effect of thermal-acoustic-air quality composite environments on overall comfort of urban pocket parks considering different landscape types. Energy and Buildings 328: 115167.

Liang Y, Yu J, Xu R, et al. (2024) Correlating working performance with thermal comfort, emotion, and fatigue evaluations through on-site study in office buildings. Building and Environment 265.

Liu S, Song R and Zhang T (2021) Residential building ventilation in situations with outdoor PM2.5 pollution. Building and Environment 202.

Liu Y, Chu C, Zhang R, et al. (2024) Impacts of high-albedo urban surfaces on outdoor thermal environment across morphological contexts: A case of Tianjin, China. Sustainable Cities and Society 100.

Luo X, Zhao Y, Yang J, et al. (2024) Adaptive design strategies for thermal comfort in waterfront campsites during summer in hot and humid regions. International Journal of Thermal Sciences 199: 108945.

McRae I, Freedman F, Rivera A, et al. (2020) Integration of the WUDAPT, WRF, and ENVI-met models to simulate extreme daytime temperature mitigation strategies in San Jose, California. Building and Environment 184.

Miao C, He X, Xu S and Chen W (2023) Vertical distribution of air pollutants in an urban street canyon during winter air pollution episodes in Shenyang, China. Building and Environment 245.

Miao C, Yu S, Hu Y, et al. (2020) Review of methods used to estimate the sky view factor in urban street canyons. Building and Environment 168.

Mobarhan M, Yeganeh M, Motie MB and Ahmadi S (2024) Assessing the efficacy of green walls versus street green lanes in mitigating air pollution: A critical evaluation. Environmental and Sustainability Indicators 24.

Mohite S and Surawar M (2024) Impact of urban street geometry on outdoor pedestrian thermal comfort during heatwave in Nagpur city. Sustainable Cities and Society 108.

Moretti E, Bonamente E, Buratti C and Cotana F (2013) Development of Innovative Heating and Cooling Systems Using Renewable Energy Sources for Non-Residential Buildings. Energies 6(10): 5114-5129.

Niu J, Zhang K, Chen J, et al. (2025) Interrelationships among physical activity, positive emotion, and thermal sensation in urban park green spaces: An empirical study in Chongqing, China. Building and Environment 270: 112567.

Qin Z, Lu B, Jing W, et al. (2024) Creating comfortable outdoor environments: Understanding the intricate relationship between sound, humidity, and thermal comfort. Urban Climate 55.

Ribeiro KFA, Justi ACA, Novais JWZ, et al. (2022) Calibration of the Physiological Equivalent Temperature (PET) index range for outside spaces in a tropical climate city. Urban Climate 44.

Salehi A and Nasrollahi N (2024) Assessing vegetation distribution based on geometrical and morphological characteristics of the urban fabric to provide thermal comfort for pedestrians: A case study in Sanandaj. Sustainable Cities and Society 104.

Sharmin T, Steemers K and Humphreys M (2019) Outdoor thermal comfort and summer PET range: A field study in tropical city Dhaka. Energy and Buildings 198: 149-159.

Shata RO, Mahmoud AH and Fahmy M (2021) Correlating the Sky View Factor with the Pedestrian Thermal Environment in a Hot Arid University Campus Plaza. Sustainability 13(2).

Su Y, Wu Z, Gao W, et al. (2024) Summer outdoor thermal comfort evaluation of urban open spaces in arid-hot climates. Energy and Buildings 321.

Wang W, Cheng X and Dai M (2022) Strategies for sustainable urban development and morphological optimization of street canyons: Measurement and simulation of PM2.5 at different points and heights. Sustainable Cities and Society 87.

Wu L, Xie B and Wang W (2022) Quantifying the impact of terrain-wind-governed close-effect on atmospheric polluted concentrations. Journal of Cleaner Production 367.

Wu S, Yu W and Chen B (2023) Observed inequality in thermal comfort exposure and its multifaceted associations with greenspace in United States cities. Landscape and Urban Planning 233.

Xiao A, Cheng B, Zhang J, et al. (2024) A study of acoustic-light-thermal effects on pedestrians' overall comfort in a Cfa-climate campus during the summer. Journal of Thermal Biology 121.

Yin Y, Luo W, Jing W, et al. (2022) Combined effects of Thermal-PM2.5 indicators on subjective evaluation of campus environment. Building and Environment 222.

Zhan Z, Jia L, Wang P and Huang L (2024) Impact of building morphology on outdoor thermal comfort in summer afternoons: A case study in Nanjing, China. Urban Climate 56: 102064.

Zhang J, Gou Z, Lu Y and Lin P (2019a) The impact of sky view factor on thermal environments in urban parks in a subtropical coastal city of Australia. Urban Forestry & Urban Greening 44: 126422.

Zhang J, Gou Z, Lu Y and Lin P (2019b) The impact of sky view factor on thermal environments in urban parks in a subtropical coastal city of Australia. Urban Forestry & Urban Greening 44.

Zhang T, Fu X, Qi F, et al. (2025a) Optimizing pedestrian thermal comfort in urban street canyons for summer and winter: Tree planting or low-albedo pavements? Sustainable Cities and Society 120.

Zhang Y, Feng S, Liu J, et al. (2025b) Campus microenvironmental factors and their effects on people's outdoor thermal perceptions under different conditions. Scientific Reports 15(1).

Zhong J, Stocker J, Cai X, et al. (2024) Street-scale air quality modelling over the West Midlands, United Kingdom: Effect of idealised traffic reduction scenarios. Urban Climate 55.

Zhu C and Lee C-C (2021) The internal and external effects of air pollution on innovation in China. Environmental Science and Pollution Research 28(8): 9462-9474.